Tumor necrosis factor-α and transforming growth factor β1 stimulate amelotin gene expression in gingival epithelial cells

（腫瘍壊死因子αおよびトランスフォーミング増殖因子β1は歯肉上皮細胞における

アメロチン遺伝子発現を促進する）

日本大学大学院松戸歯学研究科歯学専攻

高井　瑞穂

（旧姓：山﨑）

（指導：小方　賴昌　教授）

Preface

This article is based on a main paper, “Tumor necrosis factor-α stimulates human amelotin gene transcription in gingival epithelial cells” in the Inflammation Research, and a reference paper, “Amelotin gene expression is temporarily being upregulated at the initiation of apoptosis induced by TGFβ1 in mouse gingival epithelial cells” in the Apoptosis.

Abstract

Objectives: Amelotin (AMTN) is an enamel protein that is localized in the basal lamina of ameloblasts in their maturation stage and the internal basal lamina of junctional epithelium (JE) and it is suggested that AMTN could be involved in the dentogingival attachment. To elucidate the transcriptional regulation of human AMTN gene in inflamed gingiva, we have analyzed the effect of tumor necrosis factor-α (TNF-α) on the expression of AMTN gene in Ca9-22 and Sa3 human gingival epithelial cells, and to investigate the transcriptional regulation of the AMTN gene by transforming growth factor beta1 (TGFβ1) in gingival epithelial (GE1) cells in the apoptosis phase.

Materials and Methods: Total RNAs were extracted from Ca9-22, Sa3 and HSY cells after stimulation by TNF-α (10 ng/ml), and from GE1 cells treated with TGFβ1 (10 ng/ml). AMTN mRNA levels were measured by real-time PCR in Ca9-22, Sa3 and HSY cells and protein

levels by Western blotting in Ca9-22 cells. Transient transfection analyses were performed using the various lengths of AMTN gene promoter constructs with TNF-α in Ca9-22 cells, or TGFβ1 in GE1 cells. Gel mobility shift and chromatin immunoprecipitation (ChIP) assays were performed to investigate the transcription factors bindings to the human AMTN gene promoter by TNF-α.

Results: TNF-α (10 ng/ml) increased AMTN mRNA levels in Ca9-22, Sa3 and HSY cells and protein levels in Ca9-22 cells at 12 and 24 h. TNF-α induced luciferase activities of human AMTN gene promoter constructs (-211AMTN, -353AMTN and -501AMTN). TNF-α induced luciferase activities were partially inhibited in the mutation -353AMTN constructs that included 3-bp mutations in CCAAT enhancer binding protein 1 (C/EBP1), C/EBP2 and Ying Yang 1 (YY1) elements. Transcriptional activities induced by TNF-α were inhibited by protein kinase A (PKA), Src-tyrosine kinase, MEK1/2, p38 kinase, NF-κB and PI3-kinase inhibitors. Gel shift assays showed that TNF-α increased nuclear proteins binding to two types of C/EBP elements (C/EBP1 and C/EBP2) and YY1 element. The results of the chromatin immunoprecipitation assays showed that C/EBPβ binding to C/EBP1 and C/EBP2, and YY1 binding to YY1 were increased by TNF-α. Mouse AMTN mRNA levels increased at 6 h and reached maximum at 24 h in GE1 cells. Luciferase activities of the mouse AMTN gene promoter constructs were induced by TGFβ1.

Conclusion: In this study, we demonstrated that TNF-α stimulates AMTN gene transcription in human gingival epithelial cells via C/EBP1, C/EBP2 and YY1 elements in the human AMTN gene promoter. In addition, we also demonstrated that AMTN mRNA levels were induced at the initiation of apoptosis by TGFβ1 in mouse gingival epithelial cells, which could be mediated through the Smad3 signaling pathway.

Introduction

Amelotin (AMTN) is a secreted enamel protein that is transcribed mainly during the maturation stage of amelogenesis [1]. AMTN resides in the basal lamina throughout the maturation stage of ameloblasts, and is also found at the interface between the junctional epithelium (JE) and tooth enamel [2, 3]. Tooth enamel in AMTN-overexpression mice is disorganized and thin compared to wild-type mice [4], and heavy erosion and attrition of mandibular incisors were observed in AMTN-deficient mice [5]. Furthermore, it has been shown that AMTN could promote hydroxyapatite mineralization [6, 7] and it is necessary for proper enamel maturation [8], however, they focused only on amelogenesis. While the precise function of AMTN in JE is not yet known, the localization of this protein suggests that AMTN could mediate attachment between JE and tooth enamel [9, 10].

JE is a stratified, squamous, nonkeratinizing epithelium and is a specialized gingival

epithelium locating in the internal part of the marginal gingiva. In healthy periodontal tissue, JE is strongly attached to enamel surface by hemidesmosome and separate the underlying tissues from the oral cavity. Oral bacteria and the host response in periodontal disease induce apically migration of the JE and invade the gingival connective tissue with its transformation to pocket epithelium [11]. JE is the first line of defense against the constant presence of bacteria and their products, therefore the integrity of the JE is essential for maintaining a healthy periodontium [12-15]. JE synthesizes a variety of molecules directly involved in the combat against bacteria and their products [16]. The JE is a highly dynamic and adaptive tissue with a capacity for self-renewal or de novo formation, if the JE is completely removed from the tooth, the formation of a new JE occurs from basal cells of the gingival epithelium [16]. After the gingivectomy (day 5), AMTN started to appear between the cervical region of the tooth and regenerating JE [10].

Periodontitis is the main cause of missing teeth in oral diseases, generally divided into chronic and aggressive periodontitis. These two major forms of periodontitis are different in clinical pictures and molecular profiling [17-19]. Chronic periodontitis is a slowly progressive inflammatory disease, commonly found in adults and usually associated with marked accumulation of biofilm and calculus [18]. Recent investigation has demonstrated that AMTN gene expression is increased in inflamed gingiva in Japanese chronic periodontitis patients.

Inflammatory cytokines [interleukin-1β (IL-1β), interleukin-6 (IL-6) and tumor necrosis factor-α (TNF-α)] induced AMTN transcription in human gingival fibroblasts [20, 21]. *Aggregatibacter actinomycetemcomitans* is highly detected in the deep periodontal pockets of aggressive periodontitis patients, and induces apoptosis of gingival epithelial cells associated with phosphorylation of Smad2 and inhibition of Bcl2 [22, 23]. In addition, transforming growth factor beta1 (TGFβ1) induced apoptosis in gingival epithelial cells is involved in Smad2 and Erk/Akt cascade [24, 25]. Despite the facts mentioned above were already shown, the molecular mechanism of transcriptional regulation of AMTN gene in chronic or aggressive periodontitis gingiva has not been clarified. Therefore, in this study, we have analyzed the effect of TNF-α and TGFβ1 on AMTN gene transcription in human gingival epithelial cells.

Materials and Methods

Materials

Fetal calf serum (FCS), lipofectamine 2000, penicillin and streptomycin, TrypLE^{TM} Express were purchased from Invitrogen (Carlsbad, CA). PGL3-basic vector, pSV-β-galactosidase (β-Gal) control vector, PCMV5 and mitogen-activated protein kinase kinase (MEK1/2) inhibitor U0126 were obtained from Promega (Madison, WI). pCMV-SPORT6.0 Smad3

(MGC Mouse Smad3 cDNA, clone ID: 30432720) was purchased from Thermo Fisher Scientific Biosciences Corp. (Kanagawa, Japan). Protein kinase C (PKC) inhibitor H7 was from Seikagaku Corporation (Tokyo, Japan). Epidermal growth factor (EGF), protein kinase A (PKA) inhibitor KT5720, complete protease inhibitor cocktail and phenylmethylsulfonyl fluoride (PMSF) were purchased from Sigma-Aldrich Japan (Tokyo, Japan). LY249002 [phosphatidylinositol 3-kinase (PI3-K) inhibitor] and SP600125 [c-jun N-terminal kinase (JNK) inhibitor] was from Calbiochem (San Diego, CA). Triptolide [nuclear factor-kappa B (NF-κB) inhibitor] was from Tocris (Bristol, UK). SB203580 (p38 kinase inhibitor) was from Cayman Chemical (Ann Arbor, MI). PP1 (Src-tyrosine kinase inhibitor) was from Biomol Research Laboratories, Inc (Plymouth Meeting, PA). Alpha-minimum essential medium (α-MEM), Dulbecco's Modified Eagle Medium (DMEM), tyrosine kinase inhibitor herbimycin A (HA), human recombinant TNF-α, SB525334 (ALK5, TGFβR1 inhibitor) and Apoptosis *in situ* Detection Kit were purchased from Wako (Tokyo, Japan). Recombinant human transforming growth factor β1 (TGFβ1) were purchased from R&D Systems, Inc. (Minneapolis, MN, USA). SFM-101 medium was purchased from Nissui (Tokyo, Japan). ISOGEN II was purchased from Nippon Gene (Tokyo, Japan). PrimeScript RT reagent kit and SYBR Premix Ex Taq II were purchased from Takara-Bio (Tokyo, Japan). The Quickchange site-directed Mutagenesis Kit was purchased from Agilent Technologies (Santa Clara, CA).

Anti-mouse IgG (whole molecule)-peroxidase antibody produced in rabbit, Anti-rabbit IgG (whole molecule)-peroxidase antibody produced in goat and ECL prime Western Blotting Detection Reagents were purchased from GE Healthcare (Buckinghamshire, UK). All chemicals used were analytical grade.

Cell cultures

Human gingival squamous cell carcinoma-derived Ca9-22 cells and human parotid gland adenocarcinoma HSY cells or human gingival squamous cell carcinoma-derived Sa3 cells were cultured in α-MEM or DMEM supplemented with 10% FCS. Cells were first grown to confluence in 60 mm culture dishes in α-MEM or DMEM containing 10% FCS, then cultured in α-MEM or DMEM without serum for 12 h, then incubated with TNF-α for dose-response (0.1, 1, 10, and 50 ng/ml, 12 h) or for time periods (TNF-α; 10 ng/ml) extending 3 to 24 h. Mouse-derived gingival epithelial cell line (GE1) was cultured at 33 ºC in 5% CO_2 and 95% air in SFM-101 containing 1% FCS, 10 ng/ml EGF. Cells were grown to confluence in 60 mm tissue culture dishes, media were then changed to no-serum SFM-101 media for 24 h. Then GE1 cells were incubated in this media with or without TGFβ1 (10 ng/ml) by time dependent manner.

Real-time PCR

Total RNAs were extracted from triplicate cultures with ISOGEN II. They analyzed for the mRNA levels of human AMTN and glyceraldehydes-3-phosphate dehydrogenase (GAPDH) in Ca9-22, Sa3 and HSY cells, and mouse AMTN, lamininβ3 (Lamβ3), cytokeratin19 (CK19), caspase3, Smad3 and GAPDH in GE1 cells by real-time polymerase chain reaction (PCR) as described below. Total RNA (1 μg) was used as a template for cDNA synthesis. cDNA was prepared using the PrimeScript RT reagent kit. Quantitative real-time PCR was performed using the following primer sets:

human AMTN forward, 5'-GTTGAATGTACAACAGCAACTGCAC-3';

human AMTN reverse, 5'-TTCCATCCTGGACATCTGGATTA-3';

human GAPDH forward, 5'-GCACCGTCAAGGCTGAGAAC-3';

human GAPDH reverse, 5'-ATGGTGGTGAGACGCCAGT-3';

mouse AMTN forward, 5'-CTGTCAACCAGGGAACCACT-3';

mouse AMTN reverse, 5'-TGTGATGCGGTTTAGCTGAG-3';

mouse Lamβ3 forward, 5'-AGCATAGGAGCTCAGGGTGA-3';

mouse Lamβ3 reverse, 5'-AGGTTTGGTCAATCCACAGG-3';

mouse CK19 forward, 5'-GTTCAGTACGCATTGGGTCAG-3';

mouse CK19 reverse, 5'-GAGGACGAGGTCACGAAGC-3';

mouse Caspase3 forward, 5’-CTGACTGGAAAGCCGAAACTC-3’;

mouse Caspase3 reverse, 5’-CGACCCGTCCTTTGAATTTCT-3’;

mouse Smad3 forward, 5’-AGGGGCTCCC-TCACGTTATC-3’;

mouse Smad3 reverse, 5’-CATGGCCCGTAATTCATGGTG-3’;

mouse GAPDH forward, 5’-TGAAGGGGTCGTTGATGG-3’;

mouse GAPDH reverse, 5’-AAATGGTGAAGGTCGGTGTG-3’,

and the SYBR Premix Ex Taq II in a TP800 thermal cycler dice real-time system (Takara-Bio, Tokyo, Japan). The amplification reactions were performed in a final volume of 25 μl 2x SYBR Premix EX Taq (12.5 μl), 0.4 μM forward and reverse primers (0.2 μl), and 70 ng cDNA (7 μl) for human AMTN and 50 ng cDNA (5 μl) for human GAPDH, or 50 ng (5 μl) cDNA for mouse AMTN, Lamβ3, CK19, caspase3, Smad3 and 20 ng (2 μl) cDNA for mouse GAPDH. To reduce variability between replicates, PCR premixes containing all reagents except for cDNA were prepared and aliquoted into 0.2 ml PCR tubes (NIPPON Genetics, Tokyo, Japan). The thermal cycling conditions were 10 s at 95°C, 45 cycles of 5 s at 95°C and 30 s at 60°C. Post-PCR melting curves confirmed the specificity of single-target amplification, and the mRNA expressions relative to the GAPDH were determined in triplicate.

Western blotting

For Western blotting analysis, total proteins from Ca9-22 cells were separated on 12% sodium dodecyl sulfate-polyacrylamide gel electrophoresis (SDS-PAGE) and transferred to a Hybond 0.2 μm PVDF membrane. The membrane was incubated for 2 h with anti-Amelotin (ab122312; abcam, Cambridge, UK), anti-Cytokeratin 19 (ab7755; abcam) and anti-αTubulin (sc-5286; Santa Cruz Biotechnology, CA) antibodies. Anti-rabbit and anti-mouse IgG conjugated with horseradish peroxidase (HRP) were used as the secondary antibodies. Immunoreactivities were detected by ECL prime Western Blotting Detection Reagents.

Luciferase analyses

To determine the TNF-α response regions in human AMTN gene promoter, we prepared chimeric constructs by ligating human AMTN gene promoters into luciferase reporter plasmid. Various length of human AMTN gene promoter sequences (-100AMTN; -100~+60, -211AMTN; -211~+60, -353AMTN; -353~+60, -501AMTN; -501~+60, -769AMTN; -769~+60, -950AMTN; -950~+60) were prepared by PCR amplification. Then, the amplified promoter DNAs were cloned into the Sac I site of the pGL3-basic multi-cloning site. Mutation luciferase constructs, mutation CCAAT enhancer binding protein (C/EBP) 1 (-353AMTNmC/EBP1; GTGTcGGtAAgTGA), mutation C/EBP2 (-353AMTNmC/EBP2;

ACATcGGaTAgCAT), double mutation in C/EBP1 and C/EBP2 (-353AMTNmC/EBP1+mC/EBP2) and mutation Ying Yang 1 (YY1) (-353AMTNmYY1; TGcCTGCAcCcTTTTTT) were made using the Quickchange Site-directed Mutagenesis Kit within the context of the homologous -353~+60 AMTN promoter fragments. Exponentially growing Ca9-22 cells were used for the transient transfection assays. Twenty four hours after plating, the cells at 60-80% confluence were transfected using Lipofectamine 2000. The transfection mixture included 1 μg of a luciferase (LUC) construct and 1 μg β-Gal plasmid as a transfection control. Two days following transfection, the cells were cultured in α-MEM without serum for 12 h, and then stimulated with TNF-α (10 ng/ml) for 12 h prior to harvest. The luciferase activities were measured according to the supplier's protocol using a luminescence reader (AcuuFlex Lumi 400; Aloka, Tokyo, Japan). Several types of protein kinase inhibitors were used for protein kinase inhibition. Two days following transfection, the cells were deprived of serum for 12 h, and first treated with H7 (5 μM), KT5720 (100 nM), U0126 (5 μM), LY294002 (10 μM), PP1 (10 μM), Triptolide (100 nM), SB203580 (10 μM) and SP600125 (10 μM) for 30 min or HA (1 μM) for 4 h, then incubated with TNF-α (10 ng/ml) for 12 h before harvesting.

GE1 cells were used for transient transfection assays. 48 hours after plating, cells at 50~70% confluence were transfected using a Lipofectamine 2000 reagent. The transfection mixture

included 2 μg of the respective LUC construct (-116AMTN; -116~+65 mouse AMTN gene promoter, -238AMTN; -238~+65, -460AMTN; -460~+65, -705AMTN; -705~+65, -800AMTN; -878~+65, -878AMTN; -878~+65, -1651AMTN; -1651~+65, -2200AMTN; -2200~+65) and 1 μg β-Gal vector as an internal control. Two days post transfection, cells were deprived of FCS and EGF, and TGFβ1 (10 ng/ml) was added for 12 or 24 h. The luciferase activities were measured in the same as above.

Gel shift assays

Confluent Ca9-22 cells used to prepare the nuclear extracts were incubated for 3, 6 and 12 h with TNF-α (10 ng/ml) in α-MEM without serum. Double-stranded oligonucleotide encompassing the inverted CCAAT, C/EBP1, C/EBP2 and YY1 sequences in the human AMTN promoter were used as DNA probes carry a label of Cy5. 5'-Cy5-labeled oligonucleotide and complementary oligonucleotide were purchased (Sigma-Aldrich Japan, Tokyo), and they were annealed under optimal conditions (50 mM Tris-HCl pH 7.9, 10 mM $MgCl_2$). Nuclear proteins (4 μg) were incubated for 20 min at room temperature with 0.1 pM Cy5-labeled double-stranded oligonucleotide in the binding buffer containing 50 mM KCl, 0.5 mM EDTA, 10 mM Tris-HCl (pH 7.9), 1 mM dithiothreitol, 0.04% Nonidet P-40, 5% glycerol and 1 μg of poly dI-dC. After incubation, the DNA-protein complexes were separated

by electrophoresis in 6% non-denaturing acrylamide gels run at 200 V at room temperature. Following electrophoresis, the gels were analyzed using a Typhoon TRIO+ Variable Mode Imager (GE Healthcare). For competition experiments, 40-fold molar unlabeled oligonucleotides of activator protein 1 (AP1), C/EBP1, C/EBP2 and YY1 were used. The double-stranded oligonucleotide sequences were:

CCAAT For; 5'-CTAAATCCTGAATTGGTCTCTCA-3',

CCAAT Rev; 5'-TGAGAGACCAATCAGGATTTAG-3',

C/EBP1 For; 5'-AATGAAGTGTTGGGAAATGAAAAAAAA-3',

C/EBP1 Rev; TTTTTTTTCATTTCCCAACACTTCATT-3',

C/EBP2 For; 5'-TGGTAGACATTGGGTAACATAATGTC-3',

C/EBP2 Rev; 5'-GACATTATGTTACCCAATGTCTACCA-3',

YY1 For; 5'-TATTGTCTGCATCTTTTTTTAATTA-3',

YY1 Rev; 5'-TAATTAAAAAAAGATGCAGACAATA-3'.

Supershift experiments were performed using antibodies to C/EBPβ (sc-746; Santa Cruz Biotechnology) and YY1 (ChIP Grade; ab38422; abcam). Antibodies were added to each reaction mixture and incubated for 3 h before electrophoresis was performed under the same conditions as described above.

Chromatin immunoprecipitation (ChIP) assays

Ca9-22 cells were grown to confluence in 100 mm dishes (four dishes for each chromatin preparation), then cultured in serum-free α-MEM for 12 h and stimulated with TNF-α (10 ng/ml) for time periods extending from 3 to 24 h. The cells were fixed with formaldehyde for 10 min to cross-link the protein-DNA complexes. The fixed cells were rinsed twice by a wash buffer [1 mM PMSF and complete protease inhibitor cocktail in the PBS (-)] on ice, collected by scrape and centrifuged for 5 min at 4°C. The pellets were resuspended by SDS buffer (1% SDS, 0.01 M EDTA, 0.05 M Tris-HCl, pH 8.1) and sonicated to fragment the protein-DNA complexes. Sonicated cell supernatants were diluted in a 10X ChIP buffer (0.01% SDS, 1.1% Triton X-100, 1.2 mM EDTA, 16.7 mM Tris-HCl, pH8.9, 16.7 mM NaCl, 1 mM PMSF and complete protease inhibitor cocktail). The diluted supernatants were used as Input which is control contains non-specific protein-DNA complexes, and precleared with 80 μl salmon sperm DNA/Protein A-Agarose (50% Slurry) for 30 min at 4°C with gentle agitation. For the immunoprecipitation of protein-DNA complexes, 2 μg of the anti-C/EBPβ, anti-YY1-ChIP Grade and anti-Smad3 (ab28379, Abcam) antibody were used for 100 μl of precleared supernatant, incubated overnight at 4°C with rotation. The mixed solutions were added to 60 μl of salmon sperm DNA/Protein A-Agarose (50% Slurry) for 1 h at 4°C with rotation and gently centrifuged (1,000 rpm, 1 min) to pellet the antibody-histone complexes with agarose.

After removing the supernatant that contained unbound chromatin, the pellet was washed with 1 ml each of Low Salt buffer (0.1% SDS, 1% Triton X-100, 2 mM EDTA, 20 mM Tris-HCl, pH 8.1, 150 mM NaCl), High Salt buffer (0.1% SDS, 1% Triton X-100, 2 mM EDTA, 20 mM Tris-HCl, pH 8.1, 500 mM NaCl), LiCl buffer (0.25 M LiCl, 0.1% Nonidet P-40, 1% deoxycholate, 0.5 mM EDTA, 0.01 M Tris-HCl, pH 8.1), and 1 ml of TE buffer (10 mM Tris-HCl, pH 8.1, 1 mM EDTA) twice. After the TE buffer was removed, Protein A-Agarose/antibody/chromatin complexes were resuspended in a 250 µl elution buffer (1% SDS and 0.1 M $NaHCO_3$) and incubated at room temperature for 15 min with rotation. After the spin down of the agarose beads, 20 µl 5 M NaCl was added to the supernatant, incubated overnight at 65°C, and then the samples were treated with 10 µl 0.5 M EDTA, 20 µl 1 M Tris-HCl, pH 6.5, and 1 µl 10 mg/ml proteinase K for 1 h at 45°C. DNA was collected by phenol/chloroform/isoamylalcohol extraction and ethanol precipitation. The purified DNA was subjected to PCR amplification (1 cycle at 95°C, 3 min, amplification was carried out for 35 cycles, denature at 95°C, 15 s; 55 or 57°C, 15 s; 72°C, 1 min; and final extension at 72°C, 1 min) for the C/EBP1, C/EBP2 and YY1 site within the human AMTN promoter using

C/EBP1 ChIP For; 5'-AATGTCTGCAGCTAATAACC-3',

C/EBP1 ChIP Rev; 5'-GGAAACTGAGAGACCAATCA-3',

C/EBP2 ChIP For; 5'-AATTACATAAGGCCTGTCTCC-3',

C/EBP2 ChIP Rev; 5'-TTCATTAGGTGGGTTATTAGC-3',

YY1 ChIP For; 5'-GAAGAAGGAGGTGAAGAAGC-3',

YY1 ChIP Rev; 5'-CTACCATTTGAATAGAAGGTG-3' primers.

KAPA Taq^{TM} Extra HotStart was utilized for the PCR procedure and the PCR products were separated on 2% agarose gels and visualized with ultraviolet light.

Immunocytochemistry

To detect the expression of AMTN protein in GE1 cells, immunocytochemistry were carried out. Plating of GE1 cells on culture slides (Corning® BioCoat^{TM} coating with type I collagen) were stimulated by TGFβ1 (10 ng/ml) in no-serum SFM-101 media for 24 and 48 h. The cells were fixed by 4% paraformaldehyde (PFA) for 10 min at room temperature. The fixed cells were rinsed by PBS (-) twice for 5 min and a wash buffer (1xTBS solution) and blocked for 10 min. The cells were treated with anti-AMTN rabbit polyclonal antibody (1:500) [3] for 1 h, and followed by incubations with a secondary antibody for 30 min in this immunocytochemical analysis (EnVision + System HRP Labelled Polymer Anti-Rabbit, DAKO) for signal detection.

Apoptosis analysis

To investigate the apoptosis *in situ* by Smad3 overexpression, TUNEL staining was carried out using an Apoptosis in situ Detection Kit. GE1 cells were plated on culture slides (Corning® BioCoat^{TM} coating with type I collagen) and Smad3 expression vector was used at 2, 4 or 6 μg/ml in the medium. The cells were fixed by 4% PFA for 10 min at room temperature, prior to following the procedure in accordance with the manufacturer's protocol.

Statistical analysis

Triplicate samples were analyzed for each experiment, and experiments were replicated to ensure the consistency of the responses to drugs. Significant differences between control and treatment groups were determined using the Student t-test, one-way ANOVA and multiple comparison calibration (Tukey-Kramer method).

Results

Effects of TNF-α on AMTN mRNA and protein levels in Ca9-22 Cells

To elucidate the effect of TNF-α on human AMTN gene transcription, we used human gingival squamous cell carcinoma-derived epithelial-like Ca9-22 and Sa3 cells, and human parotid gland adenocarcinoma-derived epithelial-like HSY cells to express AMTN mRNA. First, the dose-response effect of TNF-α on AMTN expression was established by treating

Ca9-22 cells with different concentrations of TNF-α for 12 h. AMTN mRNA levels were increased by a maximum 10 and 50 ng/ml TNF-α (Fig. 1A). Then, 10 ng/ml TNF-α was used to determine the time-course effect on AMTN mRNA expression. TNF-α induced AMTN mRNA levels at 6 h and further increased at 12 and 24 h in Ca9-22 and Sa3 cells (Fig. 1B and C). TNF-α increased AMTN mRNA levels at 12 h and reached maximum at 24 h in HSY cells (Fig. 1D). AMTN protein levels were induced by TNF-α at 6 h and reached maximum at 12 and 24 h. Cytokeratin 19 was used as a marker of epithelial cells. TNF-α increased cytokeratin 19 protein expression at 24 h. Tubulin was used as a loading control (Fig. 1E).

Luciferase analyses of human AMTN promoter constructs

To determine the response regions of TNF-α regulated transcription in the human AMTN gene promoter, -100AMTN, -211AMTN, -353AMTN, -501AMTN, -769AMTN and -950AMTN human AMTN gene promoter constructs were transiently transfected into Ca9-22 cells and the transcriptional activities were measured in the presence or absence of TNF-α (10 ng/ml). TNF-α increased luciferase activities of -211AMTN, -353AMTN and -501AMTN constructs. Luciferase activities of -100AMTN, -769AMTN and -950AMTN constructs were not induced by TNF-α (Fig. 2). The promoter sequence between −353 to +1 of human AMTN gene contains an inverted TATA box (TCTACA; -21~-12), an inverted CCAAT box (ATTGG;

-67~-63), an AP1 (-94~-84), a C/EBP1 (-118~-105), an octamer transcription factor 1 element (Oct1, -129~ -117), a C/EBP2 (-163~-150), a YY1 (-228~-212), and a specificity protein 1 (SP1; -351~-328) (Fig. 3). To determine more precisely the target sites in the AMTN promoter through which the TNF-α (10 ng/ml) effect was being mediated, we introduced 3-bp mutations in the putative response elements targeted by TNF-α in -353AMTN (mC/EBP1, mC/EBP2 and mYY1). After introducing 3-bp mutations, the basal activities of -353AMTNmC/EBP1, -353AMTNmC/EBP2 and -353AMTNmYY1 were lower than the basal transcriptional activity of -353AMTN. Transcriptional inductions by TNF-α (10 ng/ml) were partially abrogated in -353AMTNmC/EBP1, -353AMTNmC/EBP2 and -353AMTNmYY1 (Fig. 4). When mutations were made in the pairs of C/EBP1 and C/EBP2 in -353AMTN (-353AMTNmC/EBP1+mC/EBP2) the effect of TNF-α on luciferase activity was almost totally abrogated (Fig. 4). These results suggested that C/EBP1, C/EBP2 and YY1 act as functional response elements for TNF-α regulation of AMTN gene transcription. TNF-α induced AMTN transcription was inhibited by PKA inhibitor KT5720, tyrosine kinase inhibitor HA, Src-tyrosine kinase inhibitor PP1, MEK1/2 inhibitor U0126, p38 kinase inhibitor SB203580, NF-κB inhibitor Triptolide and PI3-K inhibitor LY249002, and was not inhibited by PKC inhibitor H7 and JNK inhibitor SP600125 (Fig. 5).

Gel shift assays

To identify the nuclear proteins that bind to CCAAT, C/EBP1, C/EBP2 and YY1, and mediate TNF-α effects on transcription, Cy5-labeled double-stranded oligonucleotides were incubated with equal amounts (4 μg) of nuclear proteins extracted from Ca9-22 cells that were either not treated (Control) or treated with 10 ng/ml TNF-α for 3, 6, and 12 h. Nuclear transcription factor-Y (NF-Y) is an evolutionarily conserved trimeric transcription factor complex which specifically recognizes inverted CCAAT box [26]. When we used the inverted CCAAT as a probe, the DNA-NF-Y protein complex did not change after stimulation with 10 ng/ml TNF-α (Fig. 6, lanes 1-4). With nuclear extracts from the confluent control cultures of Ca9-22 cells, shifts of C/EBP1-, C/EBP2- and YY1-protein complexes were evident (Fig. 6, lanes 5, 9 and 13). After stimulation by 10 ng/ml TNF-α, C/EBP1-, C/EBP2- and YY1-protein complexes were increased at 3 and 6 h, and reached maximal at 12 h (Fig. 6, lanes 6-8, lanes 10-12, lanes 15-16). These DNA-protein complexes represent how specific interactions were confirmed by competition experiments in a 40-fold molar excess of C/EBP1, C/EBP2 and YY1 reduced DNA-protein complex formation (Fig. 7, lanes 3, 9 and 15). C/EBP1-protein complexes almost completely competed with C/EBP2, whereas C/EBP2-protein complexes partially competed with 40-fold molar excess of C/EBP1, suggesting that the constituents of C/EBP1- and C/EBP2-binding proteins are not the same (Fig. 7, lanes 5 and 11). AP1 did not compete

with C/EBP1- and C/EBP2-protein complexes formations (Fig. 7, lanes 4 and 10). YY1 did not compete with C/EBP1-protein complexes and slightly competed with C/EBP2-protein complexes formations (Fig. 7, lanes 6 and 12). Interestingly, AP1, C/EBP1 and C/EBP2 partially or almost completely competed with YY1-protein complexes formation (Fig. 7, lanes 16-18), suggesting that the constituents of YY1-binding proteins resemble that of AP1 and C/EBPs. To characterize the proteins in the complexes formed with C/EBP1, C/EBP2 and YY1 further, we used antibodies to C/EBPβ and YY1. The addition of C/EBPβ antibody partially disrupted the formation of the C/EBP1- and C/EBP2-protein complexes (Fig. 8, lanes 4 and 8). Anti-YY1 antibody almost completely disrupted the formation of the YY1-protein complexes (Fig. 8, lane 12).

ChIP assays

Based on the results of the luciferase assays using mutation constructs (Fig. 4), we performed a ChIP assay and examined whether C/EBP and YY1 transcription factors are able to interact directly with the human AMTN gene promoter and how TNF-α influences the interaction of these transcription factors with C/EBP1, C/EBP2 and YY1. C/EBPβ interacted with a chromatin fragment containing the C/EBP1 and C/EBP2 that were increased by TNF-α (10 ng/ml) and reached maximum at 12 and 24 h (Fig. 9). YY1 binding to YY1 element was

increased by TNF-α (10 ng/ml) and reached maximum at 12 and 24 h in Ca9-22 cells (Fig. 9). Next we investigated which signaling pathways can regulate C/EBPβ and YY1 bindings to C/EBP1, C/EBP2 and YY1 after stimulation with TNF-α, four kinds of inhibitors (KT5720, HA, U0126 and LY294002) were used with or without TNF-α treatment. When Ca9-22 cells were stimulated with TNF-α for 12h, KT5720, HA, U0126 and LY294002 almost completely inhibited C/EBPβ bindings to C/EBP1 and C/EBP2, and YY1 bindings to YY1 elements (Fig. 10A, B and C). These results suggest that TNF-α induced C/EBPβ and YY1 binding to C/EBP1, C/EBP2 and YY1 response elements in the human AMTN gene promoter via PKA, tyrosine kinase, MAPK MEK1/2 and PI3-K pathways.

Expression of AMTN, Lamβ3, CK19 and Caspase3 mRNA levels by TGFβ1 in GE1 cells

To determine the AMTN, Lamβ3, CK19 and caspase3 mRNA levels after stimulation by TGFβ1 (10 ng/ml), real-time PCR was performed using total RNA from GE1 cells. AMTN and Lamβ3 mRNA levels were significantly upregulated by TGFβ1, reached maximum at 24 h (Fig. 11A and 11B). CK19 mRNA levels were significantly decreased after stimulation by TGFβ1 at 6 h, and thereafter gradually increased and reached control levels at 48 h (Fig. 11C). CK19 expresses in JE and sulcular epithelium but not in gingival epithelium, whereas expression of Lamβ3 is localized to the JE, these findings exhibit that GE1 cells have the gene

expression profiles of not only gingival epithelium but also JE cells. Caspase3 mRNA levels were increased significantly by TGFβ1 at 48 h (Fig. 11D). These results indicated that TGFβ1 induced the AMTN, Lamβ3, and caspase3 mRNA levels in GE1 cells in agreement with the initiation of apoptosis by TGFβ1. Therefore, GE1 cells were utilized to evaluate gingival apoptosis. The other JE markers, ODAM, and FDC-SP mRNA levels did not change significantly (data not shown). AMTN protein expression were detected mostly in cytoplasm of GE1 cells and induced by TGFβ1 (Fig. 11E).

Change of AMTN expression by TGFβ1 with/without inhibitors of signaling pathways in GE1 cells

To determine the signaling pathways associated with upregulation of AMTN mRNA levels by TGFβ1 (10 ng/ml) for 24 h, we have performed real-time PCR using several inhibitors, such as KT5720 (PKA inhibitor), U0126 (ERK1/2 inhibitor), LY249002 (PI3-K/Akt inhibitor) and SB525334 (TGFβR1 inhibitor). Increased AMTN mRNA levels by TGFβ1 were almost completely inhibited by SB525334, and partially inhibited by U0126 and LY249002 (Fig. 11F). These findings suggest that the induction of AMTN by TGFβ1 in GE1 cells was mediated mainly through the Smad2/3, and partially involved in ERK 1/2 and PI3-K/Akt signaling pathways.

Transcriptional activity of mouse AMTN gene promoter by TGFβ1 and Smad3 overexpression

To investigate if AMTN gene promoter activities are correlated with the upregulation of AMTN mRNA levels by TGFβ1, transient transfection assays were performed. The results of the luciferase assays using the luciferase constructs containing AMTN gene promoter from -460 to -2200 showed that luciferase activities of -1651AMTN and -2200AMTN constructs were significantly increased by TGFβ1 (10 ng/ml, 24 h). However, no change was observed in -460AMTN, -705AMTN, or -878AMTN constructs (Fig. 12A). These findings suggested that TGFβ1 response elements might exist between -1651 and -878 base pairs upstream from the transcriptional start site in the mouse AMTN gene promoter. If we used four kinds of inhibitors (KT5720, U0126, LY249002 and SB525334) on luciferase activities of -1651AMTN with or without TGFβ1 (10 ng/ml, 24 h) stimulation, TGFβR1 inhibitor SB525334 almost completely inhibited and U0126 and LY249002 partially inhibited TGFβ1-induced -1651AMTN luciferase activities (Fig. 12B).

The effects of Smad3 on the promoter activities of mouse AMTN gene using transient transfection assays were then investigated. Transcriptional activities of -1651AMTN and -2200AMTN constructs were induced by Smad3 overexpression (Fig. 12C). These findings

suggest that the induced Smad3 after stimulation by TGFβ1 might bind to Smad-binding elements in the mouse AMTN gene promoter, and then increase in the AMTN gene transcriptions.

Upregulation of AMTN expression and induction of apoptosis by overexpression of Smad3 in GE1 cells

It is well known that TGFβ1 induces transcription factors Smad2/3 to mediate its physiological activities [23, 24]. To support the relationship between Smad3 and AMTN gene expressions after stimulation by TGFβ1, Smad3 expression vectors with or without stimulation by TGFβ1 in GE1 cells were used. Relative AMTN mRNA levels were increased by Smad3 overexpression, and further increased by TGFβ1 (Fig. 13A). Overexpression levels of Smad3 with or without stimulation by TGFβ1 were confirmed by real-time PCR (Fig. 13B). The induced apoptosis by overexpression of Smad3 (2 and 4 μg/ml) was detected by TUNEL staining (Fig. 13C).

Discussion

In this study, we first demonstrated that human AMTN gene transcription was increased by TNF-α in human gingival and parotid gland epithelial cells at the mRNA and in human

gingival epithelial cells at the protein levels (Fig. 1). In a previous study, we have shown that higher levels of gene expression for AMTN, odontogenic ameloblast-associated protein (ODAM), IL-1β and IL-6 were found in inflamed gingiva from Japanese chronic periodontitis patients [20, 21], therefore our results in this study support those findings at the cellular level. TNF-α plays a prominent role in the pathogenesis of periodontitis and seems to occupy a central position among mediators of the inflammatory cascade [27]. The production of this cytokine is started at early stages of inflammation [28], and JE is the first line of defense against microbial challenge [12-15]. AMTN protein expression in the JE was increased in *Porphyromonas gingivalis* infected mice at an early stage, whereas at later stages, AMTN protein levels were suppressed [29]. *P. gingivalis* is a major periodontopathic bacteria which causes chronic periodontitis and its lipopolysaccharide can induce production of inflammatory cytokines in the periodontium. These results suggest that the AMTN could be involved in the early antimicrobial defense mechanism and might have a role for maintaining physiological homeostasis of JE. AMTN and ODAM are novel components of the internal basal lamina [30]. AMTN interacts with itself and with ODAM, but not with other enamel proteins such as amelogenin (AMEL), ameloblastin (AMBN) and enamelin (ENAM). ODAM was found to bind to itself and with AMTN, AMBN and weakly to AMEL, but not to ENAM [31]. These results suggest that AMTN and ODAM interaction might be involved in defining the enamel

microstructure at the enamel surface.

The promoter activities of human AMTN gene were increased by TNF-α in -211AMTN, -353AMTN and -501AMTN constructs, and the increased promoter activity was highest in -353AMTN construct (Fig. 3). Therefore, we identified the highly activated regions by TNF-α were between -353 and -100 in the human AMTN gene promoter. Furthermore, the results of luciferase assays using mutation constructs demonstrate that C/EBP1, C/EBP2 and YY1 elements are essential for induction of AMTN transcription by TNF-α (Fig. 5). The nuclear proteins binding to C/EBP1, C/EBP2 and YY1 were increased by TNF-α (Fig. 7). The results of ChIP assays showed that C/EBPβ and YY1 binding to C/EBP1, C/EBP2 and YY1 were increased by TNF-α, respectively (Fig. 10). C/EBPs are a family of leucine zipper transcription factors involved in the regulation of various aspects of cellular differentiation and function in a variety of tissues [32]. C/EBPβ has a role in the mediation of inflammatory response. TNF-α promotes nuclear localization of C/EBPβ and C/EBPδ in response to inflammatory stress [33]. YY1 is a ubiquitous and multifunctional zinc-finger transcription factor member of the Polycomb-group proteins family [34]. In this study, we demonstrate that these transcription factors play important roles in transcriptional regulation of human AMTN gene.

To elucidate signaling pathways after stimulation by TNF-α, we have performed transient

transfection assays and ChIP assays using several kinase inhibitors. Luciferase activities of -353AMTN construct were significantly inhibited by KT5720, HA, U0126, LY294002, PP1, Triptolide and SB203580 (Fig. 6). The results indicate that PKA, Src-tyrosine kinase, MEK1/2, p38 kinase, NF-κB and PI3-K are involved in induction of C/EBPβ and YY1. Additionally, the results of ChIP assays confirmed the findings of luciferase assays using the kinase inhibitors (Fig. 6 and 11).

In summary, we have demonstrated that AMTN gene transcription was regulated by TNF-α in human gingival epithelial cells.

In the second study, we have investigated that the regulation of AMTN gene transcription by TGFβ1. TGFβ family members have important roles during embryonal development, growth arrest, apoptosis and epithelial-mesenchymal transition (EMT) [35]. Smad pathways are important for TGFβ signaling, whereas non-Smad TGFβ signals such as ERK, JNK, p38 kinase, PI3-K and Src kinase also exist [36]. AMTN mRNA expressions were increased by TGFβ1 at 24 h (Fig. 11A), and TGFβ1-induced AMTN mRNA levels were almost completely abrogated by TGFβR1 inhibitors (SB525334), and were partially inhibited by MEK1/2 (U0126) and PI3-K/Akt (LY294002) inhibitors, respectively (Fig. 11F). These results suggested that the TGFβ1 induced AMTN gene transcription is mediated mainly through Smad pathways, and MAPK and PI3-K/Akt signals are also partially related. We investigated

the regulation of AMTN gene expression by TGFβ1 in ameloblast-lineage cells (ALC) which have a characteristic of maturation stage of enamel formation [37], however the AMTN mRNA levels in ALC were very low (data not shown). Smads exert their activities by interacting with specific DNA response elements together with other transcription factors [38]. Smad3, but not Smad2, can bind to the Smad-binding element (AGAC or GTCT) called SBE [39]. Furthermore, the effects of Smad3 on the regulation of AMTN gene transcription were examined using Smad3 overexpression vector. AMTN mRNA levels and transcriptional activities of -1651AMTN and -2200AMTN constructs were increased by TGFβ1 and Smad3 overexpression. On the other hand, no change was observed in -878AMTN constructs (Fig. 12A and 12C).

It has been shown that the remarkable relationship between Smad signaling associated with TGFβ1 and gingival epithelium. Smad2-deficient mice showed delayed wound healing due to the inhibition of epithelial cell migration at the early stage [40]. In addition, the acceleration of palatal wound closure in Smad3-/- mice was supported by an increase in keratinocytes and dermal cell proliferation at the wound sites [41]. These reports did not show the expression levels of JE relative genes including AMTN. However, TGFβ and Smad2/Smad3 signaling pathways are crucial for migration and proliferation of epithelial cells for the homeostasis and wound healing of epithelium.

In these studies, we have characterized the highly activated region in the human AMTN gene promoter which is required for transcriptional regulation by TNF-α and revealed that the region contains C/EBP1, C/EBP2 and YY1 elements. Moreover, TNF-α increased C/EBPβ and YY1 binding to these elements via PKA, Src-tyrosine kinase, MEK1/2, p38 kinase, NF-κB and PI3-K pathways. AMTN gene expression was temporarily upregulated at the initiation of apoptosis induced by TGFβ1 in mouse gingival epithelial cells. Therefore, in the gingival epithelia, AMTN might have an important role to maintain the homeostasis of periodontium.

References

1. Iwasaki K, Bajenova E, Somogyi-Ganss E, Miller M, Nguyen V, Nourkeyhani H, Gao Y, Wendel M, Ganss B. Amelotin - a Novel Secreted, Ameloblast-specific Protein. J Dent Res. 2005; 84: 1127-1132.
2. Moffatt P, Smith CE, St-Arnaud R, Simmons D, Wright JT, Nanci A. Cloning of rat amelotin and localization of the protein to the basal lamina of maturation stage ameloblasts and junctional epithelium. Biochem J. 2006; 399: 37-46.
3. Somogyi-Ganss E, Nakayama Y, Iwasaki K, Nakano Y, Stolf D, McKee MD, Ganss B. Comparative temporospatial expression profiling of murine amelotin protein during

amelogenesis. Cells Tissues Organs. 2012; 195: 535-549.

4. Lacruz RS, Nakayama Y, Holcroft J, Nguyen V, Somogyi-Ganss E, Snead ML, White SN, Paine ML, Ganss B. Targeted overexpression of amelotin disrupts the microstructure of dental enamel. PLoS One. 2012; 7(4): e35200.
5. Nakayama Y, Holcroft J, Ganss B. Enamel Hypomineralization and Structural Defects in Amelotin-deficient Mice. J Dent Res. 2015; 94: 697-705.
6. Gasse B, Silvent J, Sire JY. Evolutionary analysis suggests that AMTN is enamel-specific and a candidate for AI. J Dent Res. 2012; 91: 1085-1089.
7. Abbarin N, San Miguel S, Holcroft J, Iwasaki K, Ganss B. The enamel protein amelotin is a promoter of hydroxyapatite mineralization. J Bone Miner Res. 2015; 30: 775-785.
8. Núñez SM, Chun YH, Ganss B, Hu Y, Richardson AS, Schmitz JE, Fajardo R, Yang J, Hu JC, Simmer JP. Maturation stage enamel malformations in Amtn and Klk4 null mice. Matrix Biol. 2016; 52-54: 219-233.
9. Ganss B, Abbarin N. Maturation and beyond: proteins in the developmental continuum from enamel epithelium to junctional epithelium. Front Physiol. 2014; 5: 371.
10. Nishio C, Wazen R, Kuroda S, Moffatt P, Nanci A. Expression pattern of odontogenic ameloblast-associated and amelotin during formation and regeneration of the junctional epithelium. Eur Cell Mater. 2010; 20: 393-402.

11. Lee HK, Ji S, Park SJ, Choung HW, Choi Y, Lee HJ, Park SY, Park JC. Odontogenic ameloblast-associated protein (ODAM) mediates junctional epithelium attachment to teeth via integrin-ODAM-Rho guanine nucleotide exchange factor 5 (ARHGEF5)-RhoA signaling. J Biol Chem. 2015; 290: 14740-14753.
12. Schroeder HE, Listgarten MA. The gingival tissues: the architecture of periodontal protection. Periodontol 2000. 1997; 13: 91-120.
13. Schroeder HE, Listgarten MA. The junctional epithelium: from strength to defense. J Dent Res. 2003; 82: 158-161.
14. Hormia M, Owaribe K, Virtanen I. The dento-epithelial junction: cell adhesion by type I hemidesmosomes in the absence of a true basal lamina. J Periodontol. 2001; 72: 788-797.
15. Nishio C, Wazen R, Moffatt P, Nanci A. Expression of odontogenic ameloblast-associated and amelotin proteins in the junctional epithelium. Periodontol 2000. 2013; 63: 59-66.
16. Bosshardt DD, Lang NP. The junctional epithelium: from health to disease. J Dent Res. 2005; 84: 9-20.
17. Kebschull M, Demmer RT, Grün B et al. Gingival tissue transcriptomes identify distinct periodontitis phenotypes. J Dent Res 2014; 93: 459-468.
18. Duarte PM, Bastos MF, Fermiano D et al. Do subjects with aggressive and chronic periodontitis exhibit a different cytokine/chemokine profile in the gingival crevicular

fluid? A systematic review. J Periodontal Res 2015; 50: 18-27.

19. Kebschull M, Guarnieri P, Demmer RT et al. Molecular differences between chronic and aggressive periodontitis. J Dent Res 2013; 92: 1081-1088.

20. Nakayama Y, Takai H, Matsui S, Matsumura H, Zhou L, Kato A, Ganss B, Ogata Y. Proinflammatory cytokines induce amelotin transcription in human gingival fibroblasts. J Oral Sci. 2014; 56 :261-268.

21. Nakayama Y, Takai H, Matsui S, Zhou L, Abiko Y, Ganss B, Ogata Y. Transcriptional regulation of amelotin gene by proinflammatory cytokines in gingival fibroblasts. Connect Tissue Res. 2014; 55 Suppl 1 :18-20.

22. Yoshimoto T, Fujita T, Ouhara K et al. Smad2 is involved in Aggregatibacter actinomycetemcomitans-induced apoptosis. J Dent Res 2014; 93:1148-1154.

23. Fujita T, Alotaibi M, Kitase Y et al. Smad2 is involved in the apoptosis of murine gingival junctional epithelium associated with inhibition of Bcl-2. Arch Oral Biol 2012; 57:1567-1573.

24. Lu H, Mackenzie IC, Levine AE. Transforming growth factor-beta response and expression in junctional and oral gingival epithelial cells. J Periodontal Res 1997; 32: 682-691.

25. Yoshimoto T, Fujita T, Kajiya M et al. Involvement of smad2 and Erk/Akt cascade in

TGF-β1-induced apoptosis in human gingival epithelial cells. Cytokine 2015; 75: 165-173.

26. Shimizu E, Ogata Y. Activation of bone sialoprotein gene transcription by flavonoids is mediated through an inverted CCAAT box in ROS 17/2.8 cells. J Cell Biochem. 2002; 86:35-44.

27. Yucel-Lindberg T, Båge T. Inflammatory mediators in the pathogenesis of periodontitis. Expert Rev Mol Med. 2013; 15 :e7.

28. Hopkins SJ. The pathophysiological role of cytokines. Leg Med (Tokyo). 2003; 5 Suppl 1: S45-57.

29. Nakayama Y, Kobayashi R, Matsui S, Matsumura H, Iwai Y, Noda K, Yamazaki M, Kurita-Ochiai T, Yoshimura A, Shinomura T, Ganss B, Ogata Y. Localization and expression pattern of amelotin, odontogenic ameloblast-associated protein and follicular dendritic cell-secreted protein in the junctional epithelium of inflamed gingiva. Odontology. 2017; 105:329-337.

30. Dos Santos Neves J, Wazen RM, Kuroda S, Francis Zalzal S, Moffatt P, Nanci A. Odontogenic ameloblast-associated and amelotin are novel basal lamina components. Histochem Cell Biol. 2012; 137: 329-338.

31. Holcroft J1, Ganss B. Identification of amelotin- and ODAM-interacting enamel matrix

proteins using the yeast two-hybrid system. Eur J Oral Sci. 2011; 119 Suppl 1 :301-306.

32. Poli V. The role of C/EBP isoforms in the control of inflammatory and native immunity functions. J Biol Chem. 1998; 273: 29279-29282.

33. Lekstrom-Himes J, Xanthopoulos KG. Biological role of the CCAAT/enhancer-binding protein family of transcription factors. J Biol Chem. 1998 ;273: 28545-28548.

34. Gordon S, Akopyan G, Garban H, Bonavida B. Transcription factor YY1: structure, function, and therapeutic implications in cancer biology. Oncogene. 2006; 25: 1125-1142.

35. Heldin CH, Landström M, Moustakas A. Mechanism of TGF-beta signaling to growth arrest, apoptosis, and epithelial-mesenchymal transition. Curr Opin Cell Biol 2009; 21:166-176.

36. Moustakas A, Heldin CH. Non-Smad TGF-beta signals. J Cell Sci 2005; 118(Pt 16):3573-3584.

37. Nakata A, Kameda T, Nagai H, Ikegami K, Duan Y, Terada K, Sugiyama T. Establishment and characterization of a spontaneously immortalized mouse ameloblast-lineage cell line. Biochem Biophys Res Commun 2003; 308: 834-839.

38. Shi Y, Massagué J. Mechanisms of TGF-beta signaling from cell membrane to the nucleus. Cell 2003; 113: 685-700.

39. Chai J, Wu JW, Yan N et al. Features of a Smad3 MH1-DNA complex. Roles of water and

zinc in DNA binding. J Biol Chem 2003; 278:20327-20331.

40. Tomikawa K, Yamamoto T, Shiomi N et al. Smad2 decelerates re-epithelialization during gingival wound healing. J Dent Res 2012; 91:764-770.

41. Jinno K, Takahashi T, Tsuchida K et al. Acceleration of palatal wound healing in Smad3-deficient mice. J Dent Res 2009; 88:757-761.

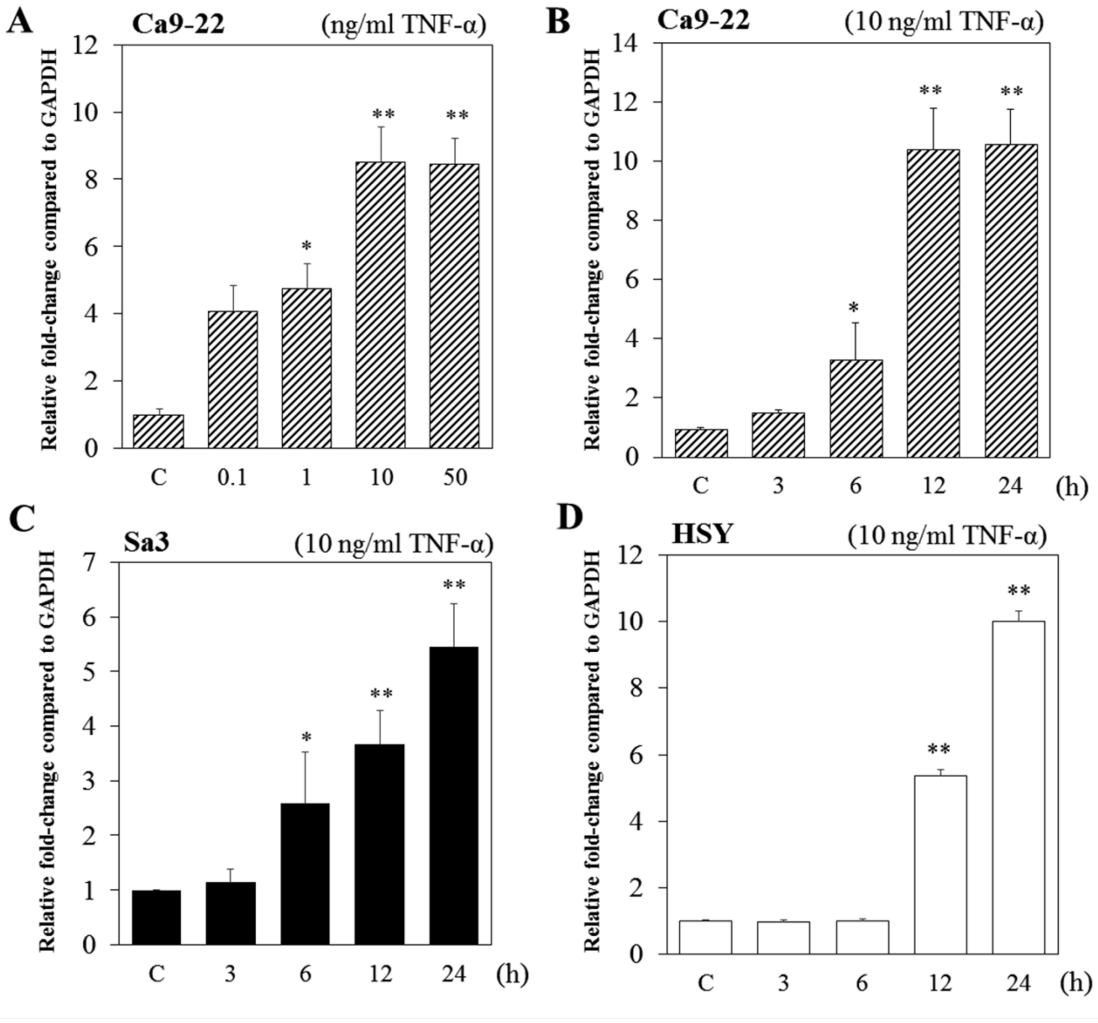
A
Ca9-22
(ng/ml TNF-α)
Relative fold-change compared to GAPDH
C
0.1
1
10
50
B
Ca9-22
(10 ng/ml TNF-α)
Relative fold-change compared to GAPDH
C
3
6
12
24
(h)
C
Sa3
(10 ng/ml TNF-α)
Relative fold-change compared to GAPDH
C
3
6
12
24
(h)
D
HSY
(10 ng/ml TNF-α)
Relative fold-change compared to GAPDH
C
3
6
12
24
(h)

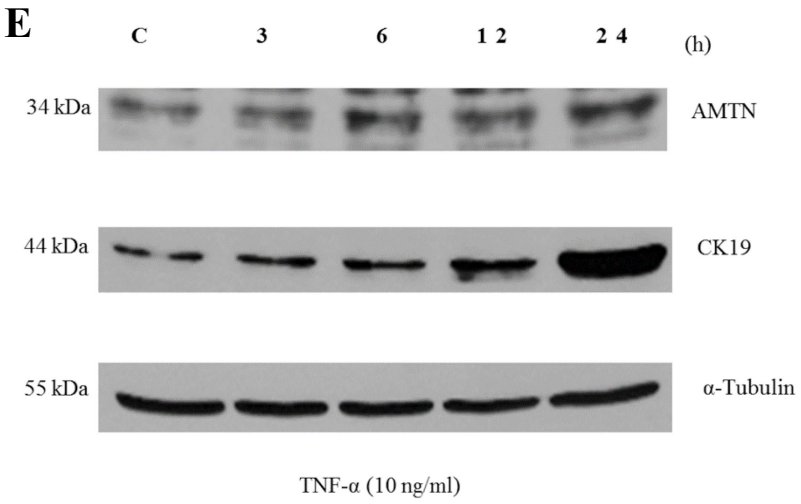
E
C
3
6
12
24
(h)
34 kDa
AMTN
44 kDa
CK19
55 kDa
α-Tubulin
TNF-α (10 ng/ml)

Fig. 1 Effects of TNF-α on AMTN mRNA levels in Ca9-22, Sa3 and HSY cells. **A:** Dose-response effects of TNF-α on AMTN mRNA levels in Ca9-22 cells treated for 12 h. **B:** Ca9-22 cells were treated with or without TNF-α (10 ng/ml) for 3, 6, 12, and 24 h. **C:** Sa3 cells were treated with or without TNF-α (10 ng/ml) for 3, 6, 12, and 24 h. **D:** HSY cells were treated with or without TNF-α (10 ng/ml) for 3, 6, 12, and 24 h. AMTN and GAPDH mRNA levels were measured by real-time PCR. The experiments were performed in triplicate for each data point. Quantitative analyses of the data sets are shown with standard errors. Significantly different from control; *P<0.05 and *P<0.01. **E:** Effects of TNF-α on AMTN protein levels in Ca9-22 cells. AMTN protein levels in Ca9-22 cells were analyzed by Western blotting using an anti-AMTN, anti-CK19 and an anti-α tubulin antibodies.

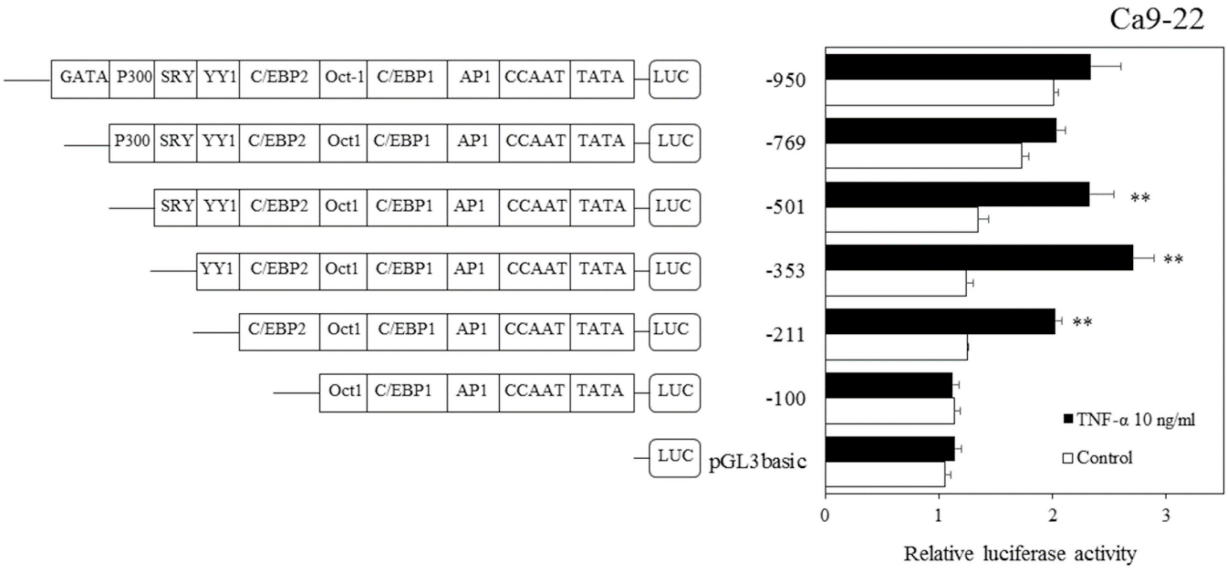

Fig. 2 TNF-α upregulates human AMTN gene promoter activities. The transcriptional activities of -211AMTN (-211~+60), -353AMTN (-353~+60) and -501AMTN (-501~+60) were increased by TNF-α (10 ng/ml, 12 h) in Ca9-22 cells. Results of transcriptional activities obtained from three separate transfections with constructs, pGL3-basic and -100AMTN to -950AMTN were combined and values expressed with standard errors. *P<0.05 and **P<0.01

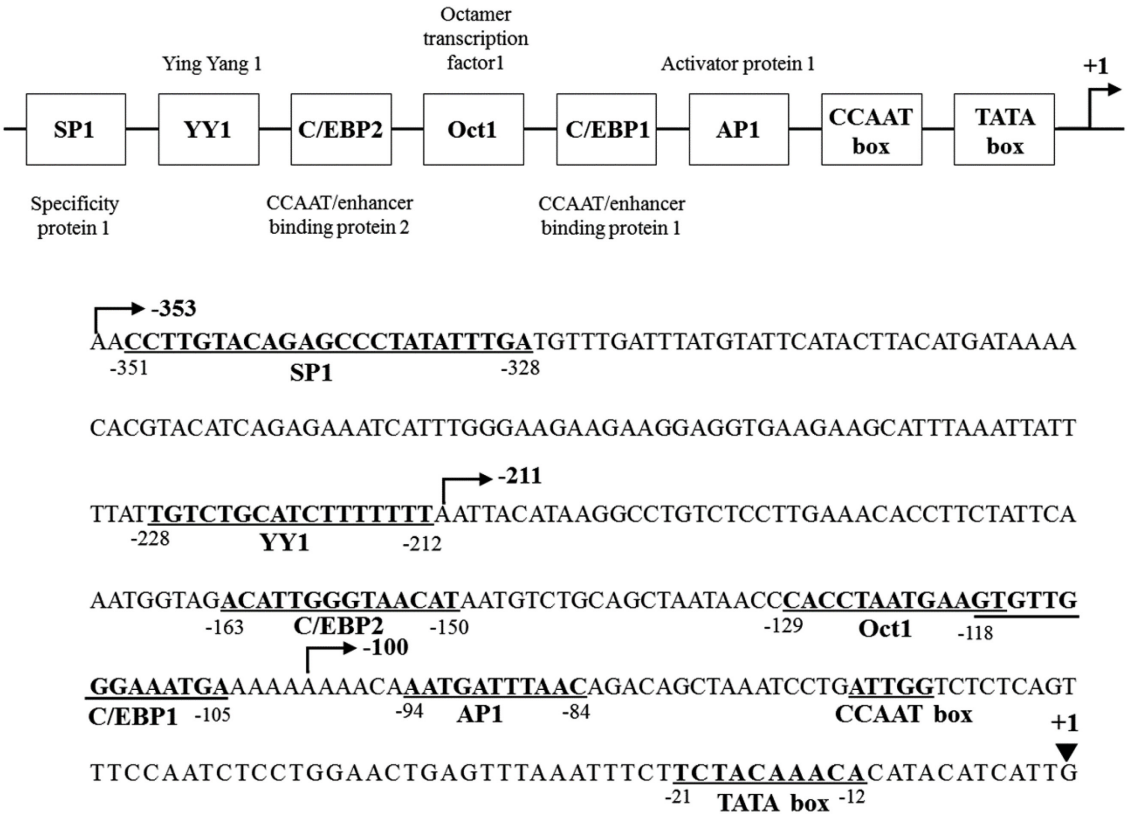

Fig. 3 Regulatory elements in the proximal promoter of the human AMTN gene. **Upper panel:** The schematic diagram of human AMTN gene proximal promoter. **Lower panel:** The nucleotide sequence of the human AMTN gene proximal promoter from -353 to transcription start point. An inverted TATA box, inverted CCAAT box, AP1, C/EBP1, Oct1, C/EBP2, YY1 and SP1 are present.

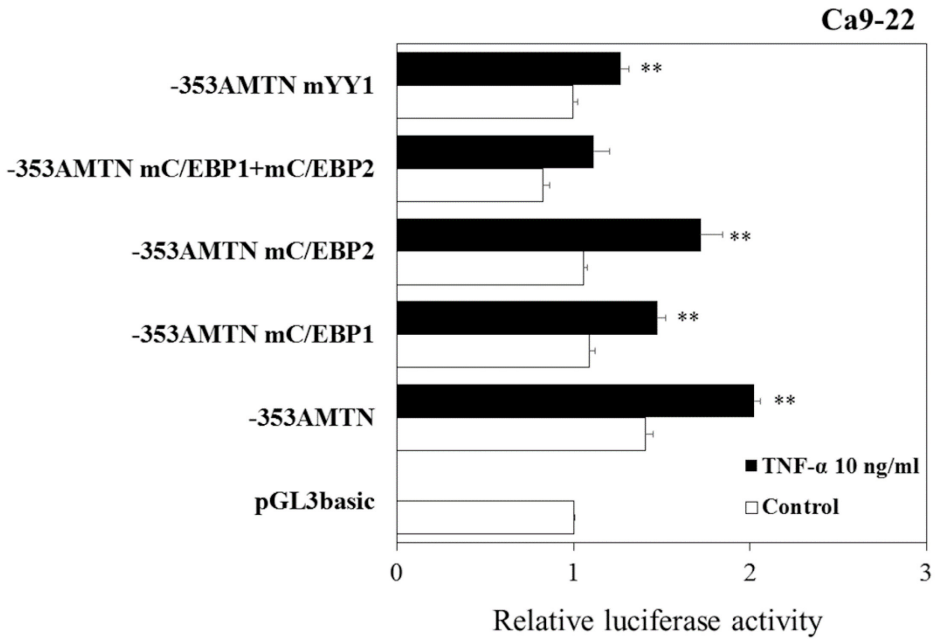

Fig. 4 Site-specific mutation analyses of luciferase activities in Ca9-22 cells. After introducing 3-bp mutations, transcriptional induction by TNF-α (10 ng/ml) was partially inhibited in the -353AMTNmC/EBP1, -353AMTNmC/EBP2 and -353AMTNmYY1. Double mutation in C/EBP1 and C/EBP2 (-353AMTNmC/EBP1+mC/EBP2) almost completely abolished the effect of TNF-α. The results of transcriptional activities obtained from three separate transfections with constructs were combined and the values were expressed with standard errors. Significantly different from control, *P<0.05 and **P<0.01.

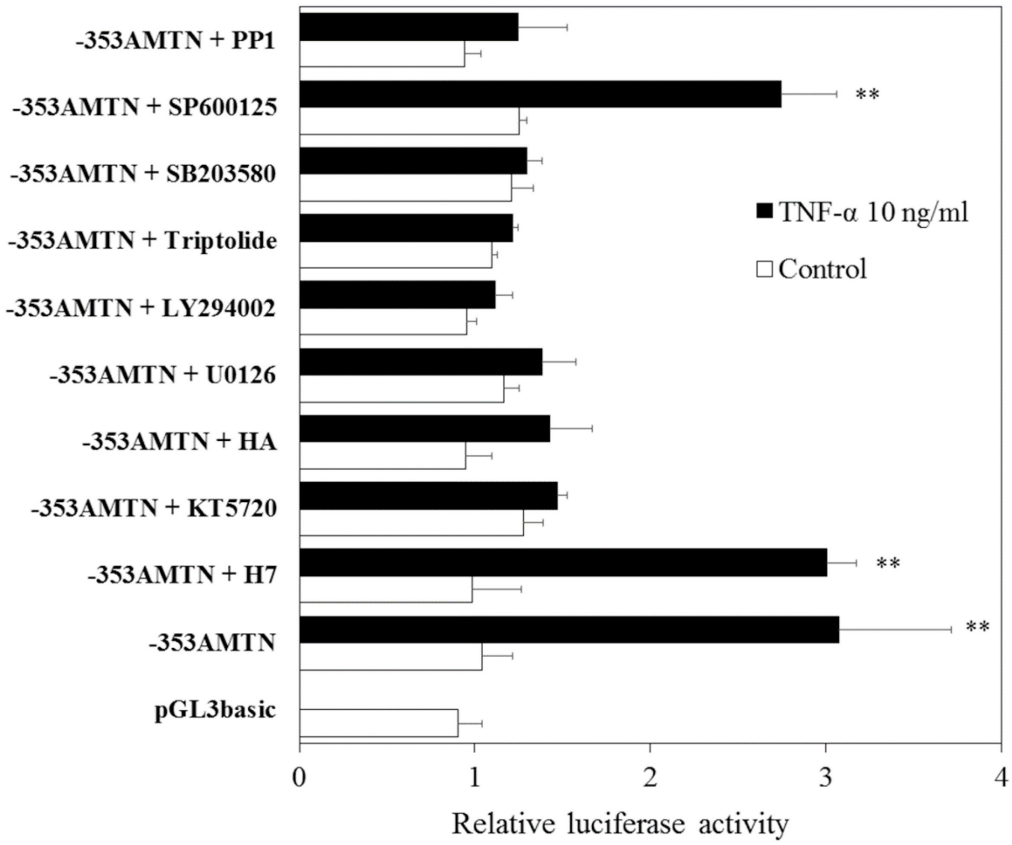

Fig. 5 Effects of kinase inhibitors on transcriptional activation by TNF-α. TNF-α-induced -353AMTN activities were inhibited by KT5720, HA, PP1, U0126, SB203580, Triptolide and LY294002, and no effect was observed for H7 and SP600125. The results of transcriptional activities obtained from three separate transfections with constructs were combined and values expressed with standard errors. Significantly different from control, *P<0.05 and **P<0.01.

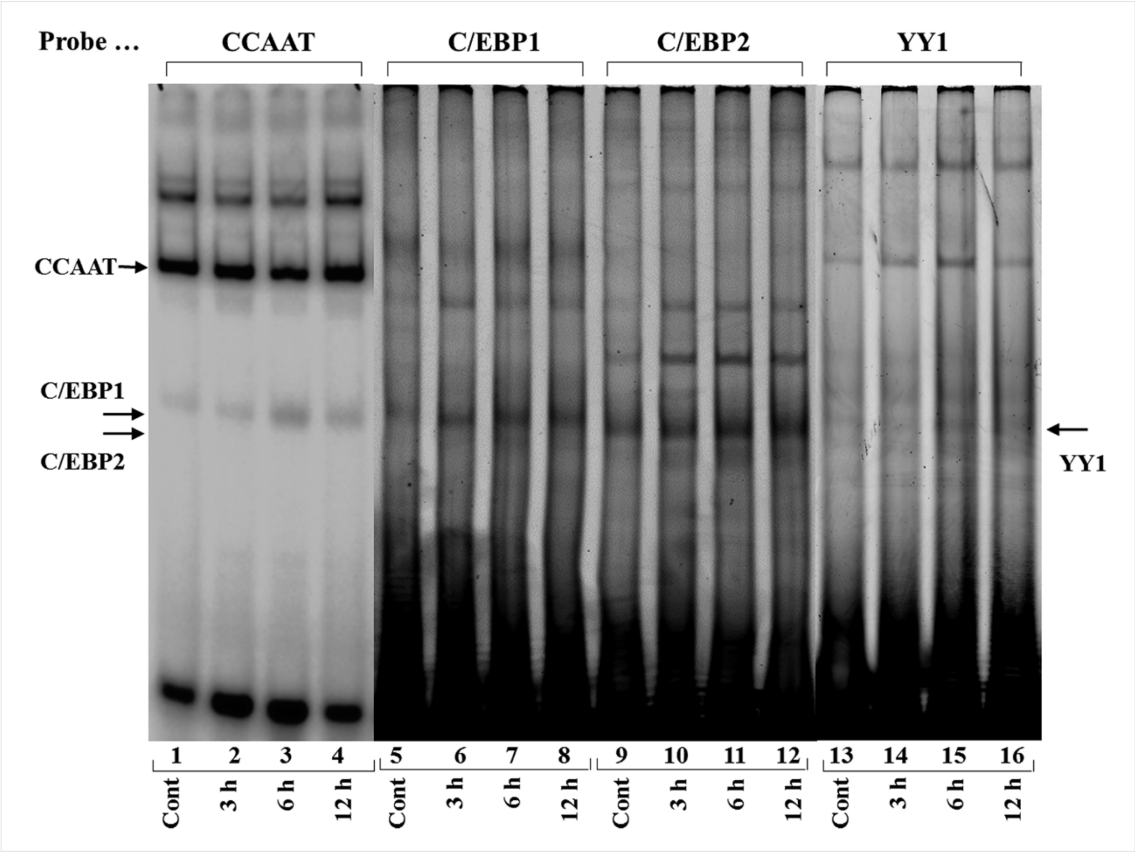

Fig. 6 Gel mobility shift assays using CCAAT, C/EBP1, C/EBP2 and YY1. Cy5-labeled double-stranded CCAAT, C/EBP1, C/EBP2 and YY1 oligonucleotides were incubated with nuclear proteins obtained from Ca9-22 cells stimulated with TNF-α (10 ng/ml). DNA-protein complexes were loaded on 6% polyacrylamide gel and analyzed by using an imaging system.

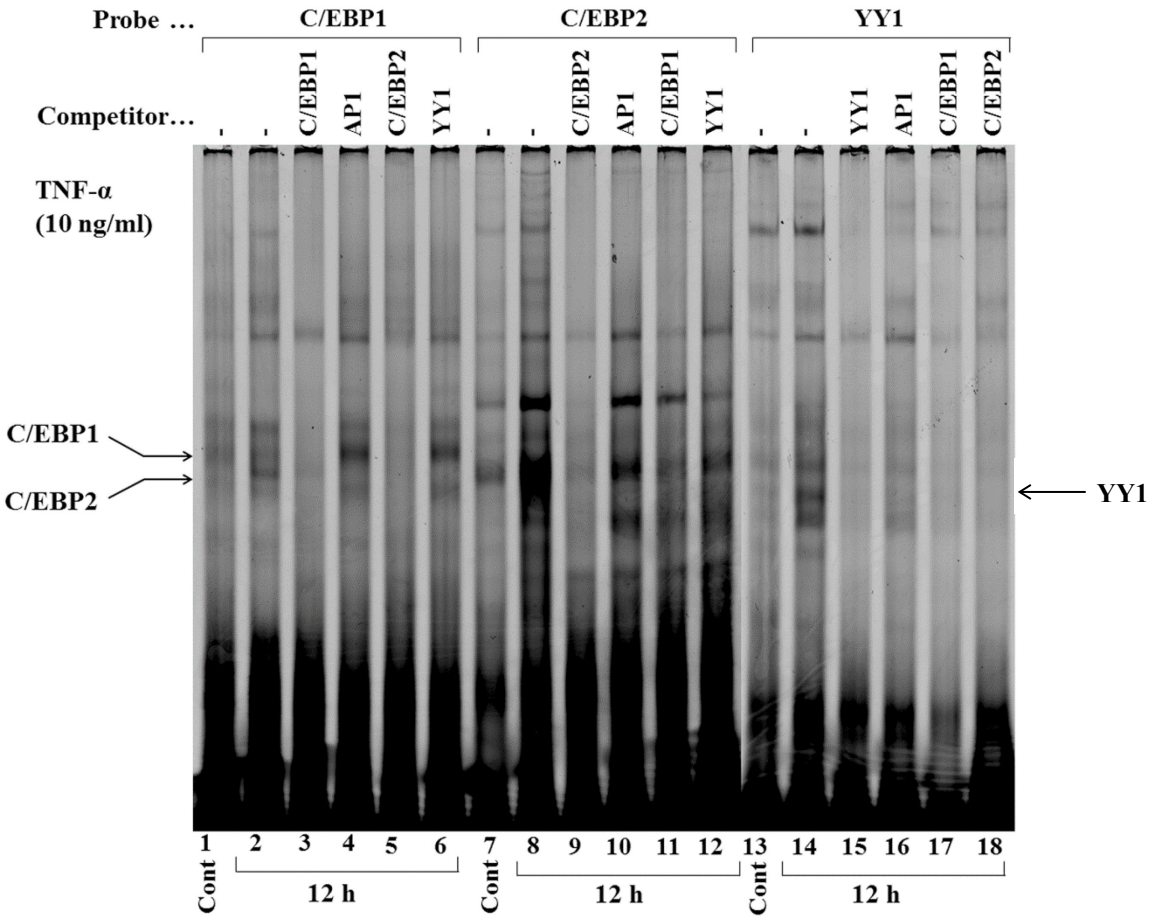

Fig. 7 Specific binding of nuclear proteins to C/EBP1, C/EBP2 and YY1. Competition assays were performed using 40-fold molar unlabeled oligonucleotides for AP1, C/EBP1, C/EBP2 and YY1. DNA-protein complexes were loaded on 6% polyacrylamide gel and analyzed using an imaging system.

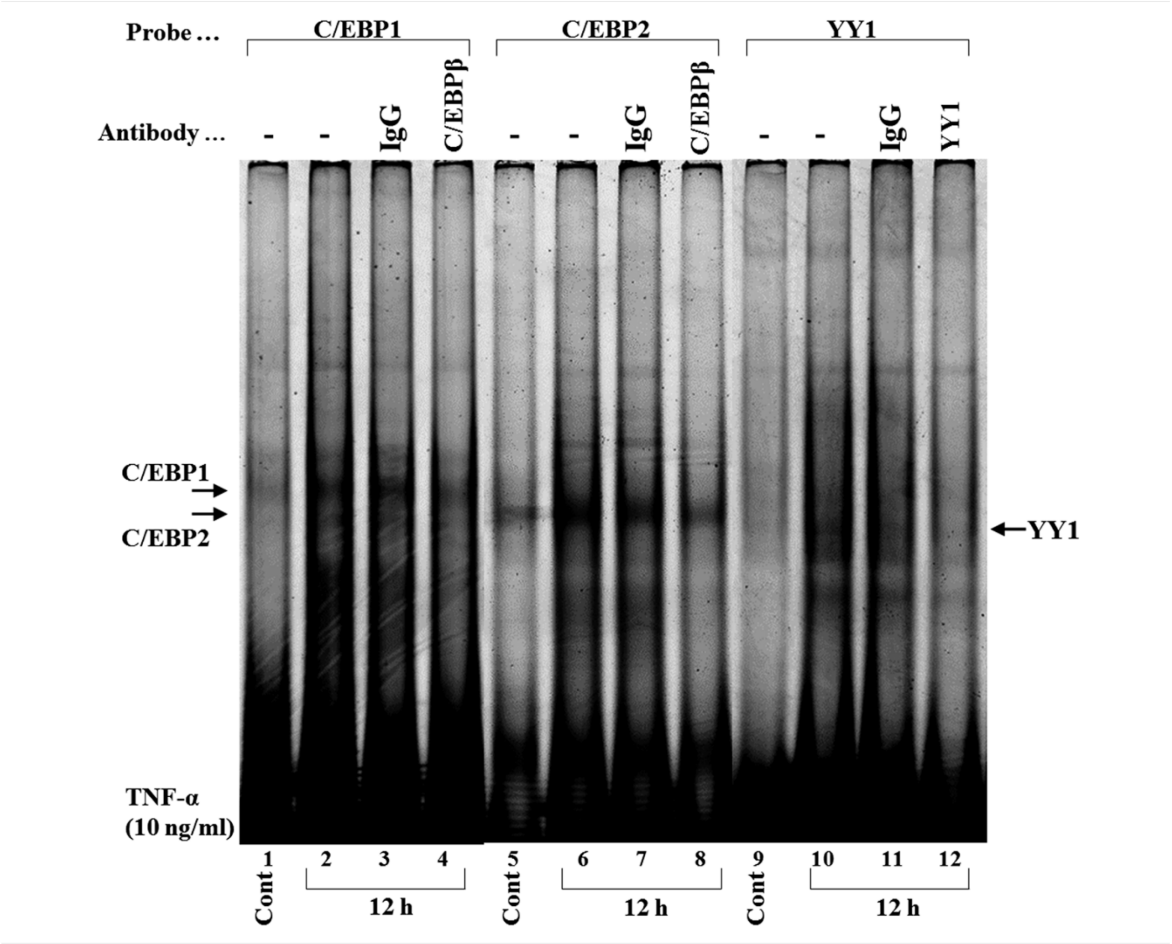

Fig. 8 Supershift assays using antibodies to C/EBPβ and YY1. Supershift experiments were performed with 0.4 μg of antibodies against C/EBPβ and YY1 added separately to each gel shift reaction, DNA-protein complexes were separated by electrophoresis through a 6% polyacrylamide gel and analyzed by using an imaging system.

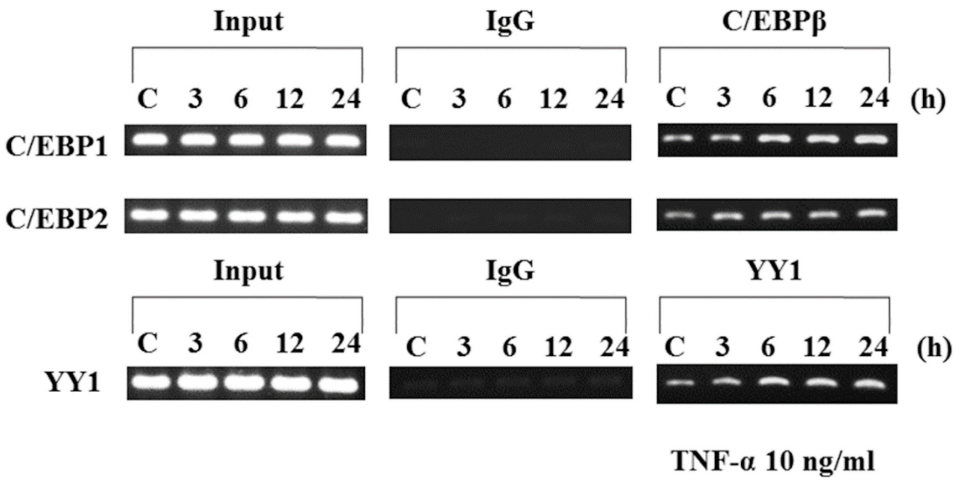

Fig. 9 ChIP analyses of transcription factors binding to C/EBP1, C/EBP2 and YY1 in the human AMTN gene promoter in Ca9-22 cells. PCR bands amplified and corresponding to DNA-protein complexes immunoprecipitated with antibodies showed that C/EBPβ and YY1 interacted with a chromatin fragment containing the C/EBP1, C/EBP2 and YY1, which were increased in Ca9-22 cells following stimulation with TNF-α.

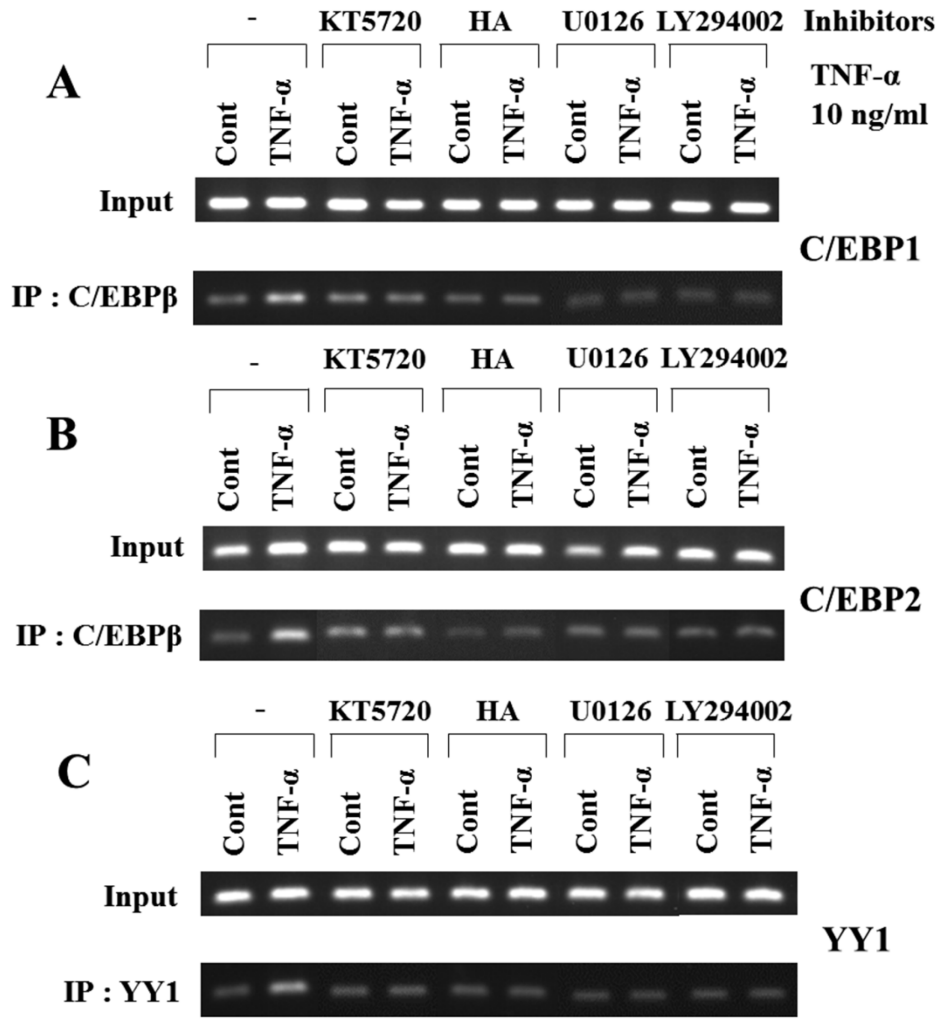

Fig. 10 ChIP analyses of transcription factors binding to C/EBP1, C/EBP2 and YY1 under the treatment by TNF-α (10 ng/ml) with kinase inhibitors. Treatments of KT5720, HA, U0126 and LY294002 almost completely abolished the induction of C/EBPβ and YY1 bindings to C/EBP1, C/EBP2 and YY1 following stimulation with TNF-α.

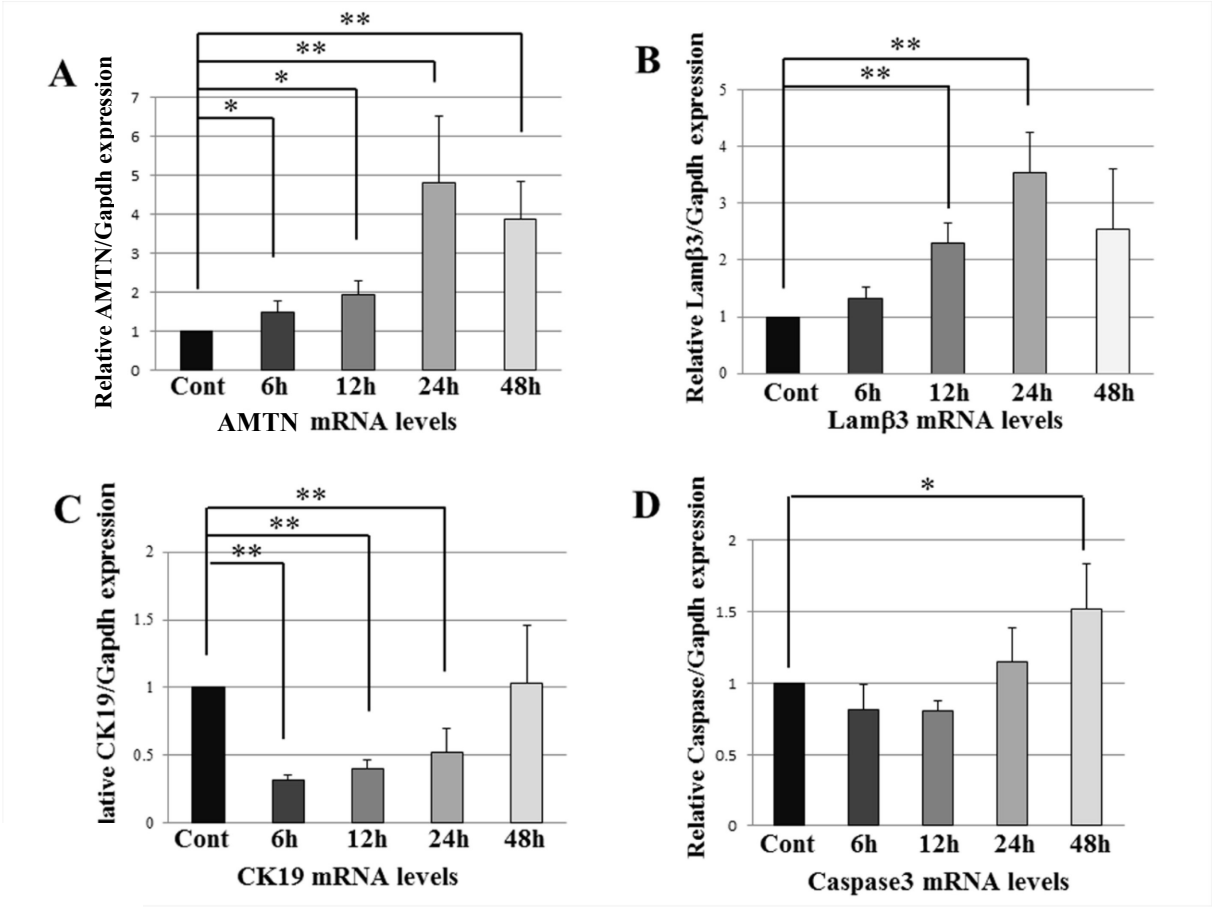
A
Relative AMTN/Gapdh expression
AMTN mRNA levels
Cont
6h
12h
24h
48h
B
Relative Lamβ3/Gapdh expression
Lamβ3 mRNA levels
C
lative CK19/Gapdh expression
CK19 mRNA levels
D
Relative Caspase/Gapdh expression
Caspase3 mRNA levels

E

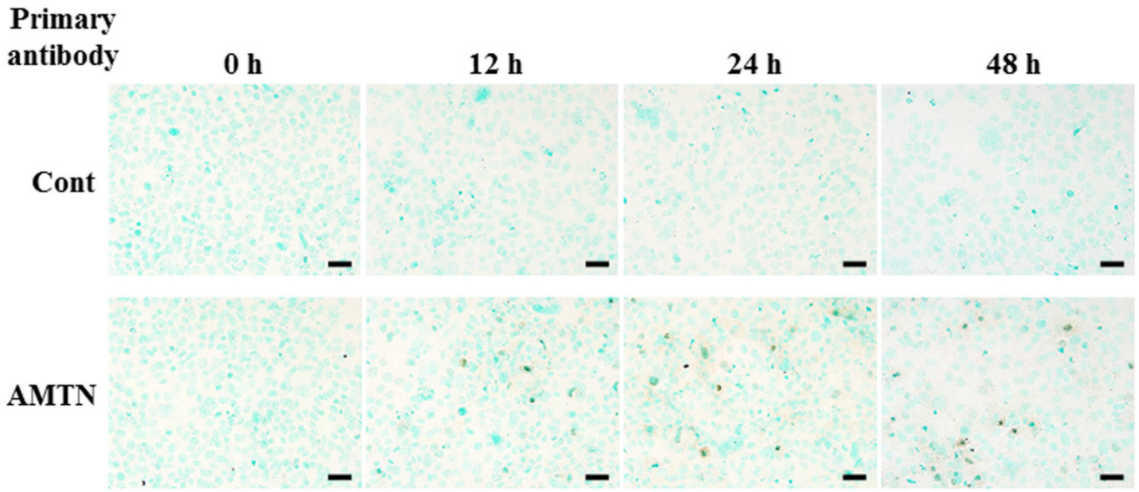
Primary antibody
0 h
12 h
24 h
48 h
Cont
AMTN

F

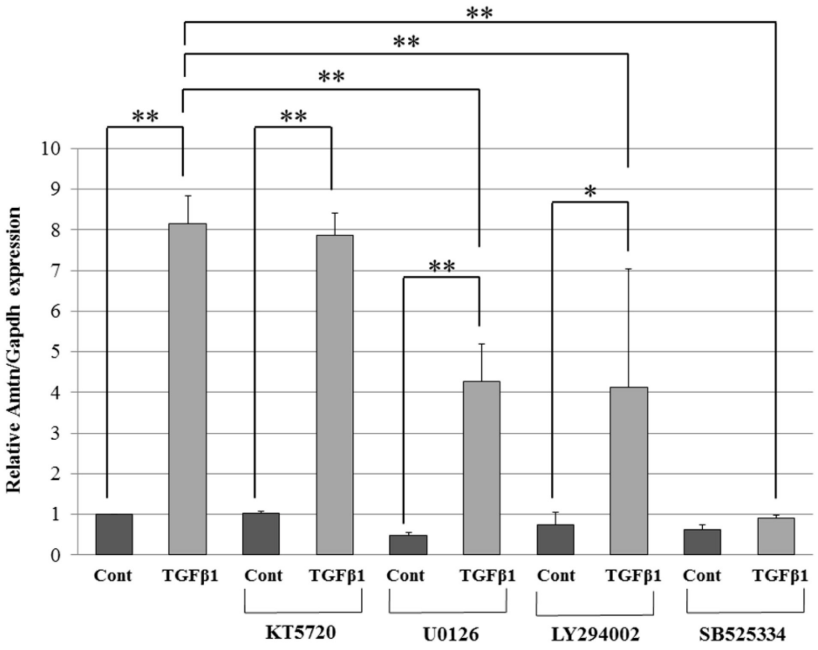

Fig. 11 TGFβ1 regulation of AMTN, Lamβ3, CK19 and Caspase 3 mRNA levels in GE1 cells. **A-D:** Time course effects of TGFβ1 (10ng/ml) on AMTN (A), Lamβ3 (B), CK19 (C) and Caspase3 (D) mRNA levels in GE1 cells. Quantitative analyses of the data sets are shown with standard deviation. Significantly different from control. **E:** Immunocytochemical staining showed that AMTN protein expression levels were induced by TGFβ1 (10 ng/ml) at 24 h, and reached at maximal levels by TGFβ1 (10 ng/ml) at 48 h. (Cont: non-primary antibodies, counter staining with Methyl green, Bar: 20 μm). **F:** AMTN mRNA levels were completely blocked by SB525334 (1 μM), and partially inhibited by U0126 (5 μM) and LY249002 (10 μM). KT5750 (100 nM) had no effect on the level of AMTN mRNA (**P* <0.05, ***P* <0.01).

A

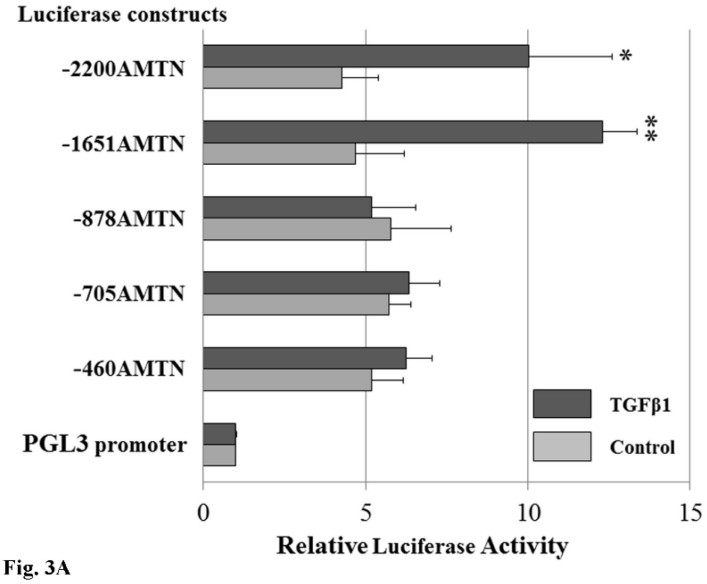

Fig. 3A

B

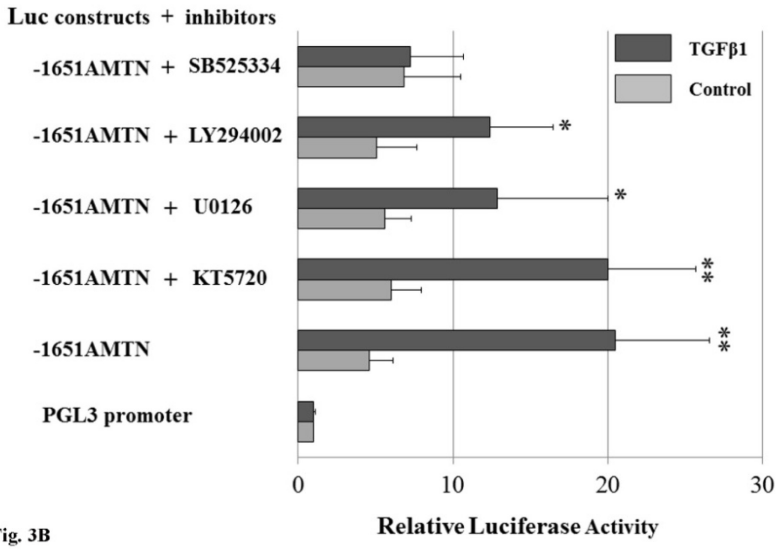

Fig. 3B

C

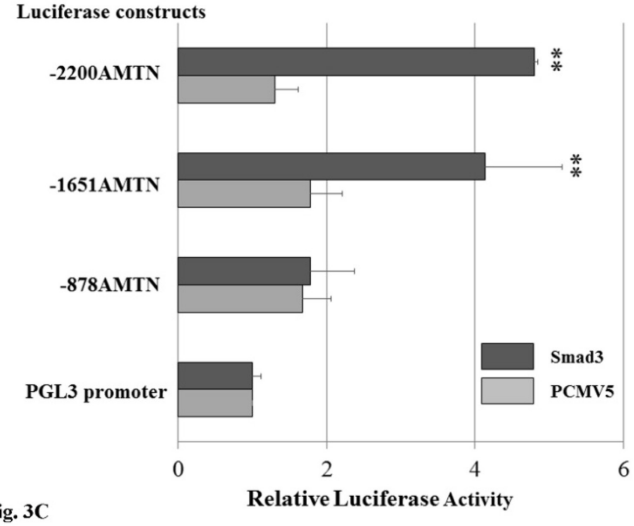

Fig. 3C

Fig. 12 TGFβ1 upregulated transcriptional activities of the mouse AMTN gene promoter. **A:** Transcriptional activities of -1651AMTN (-1651 to +65) and -2200AMTN (-2200 to +65) luciferase constructs were increased by TGFβ1 (10 ng/ml) at 24 h in GE1 cells. **B:** Transcriptional activity of -1651AMTN luciferase construct was completely blocked by SB525334, and partially inhibited by U0126 and LY249002. **C:** Smad3 overexpression (2 μg/ml) induced the transcriptional activities of the mouse AMTN gene promoter at the constructs of -1651AMTN (-1651 to +65) and -2200AMTN (-2200 to +65) (*P <0.05, **P <0.01).

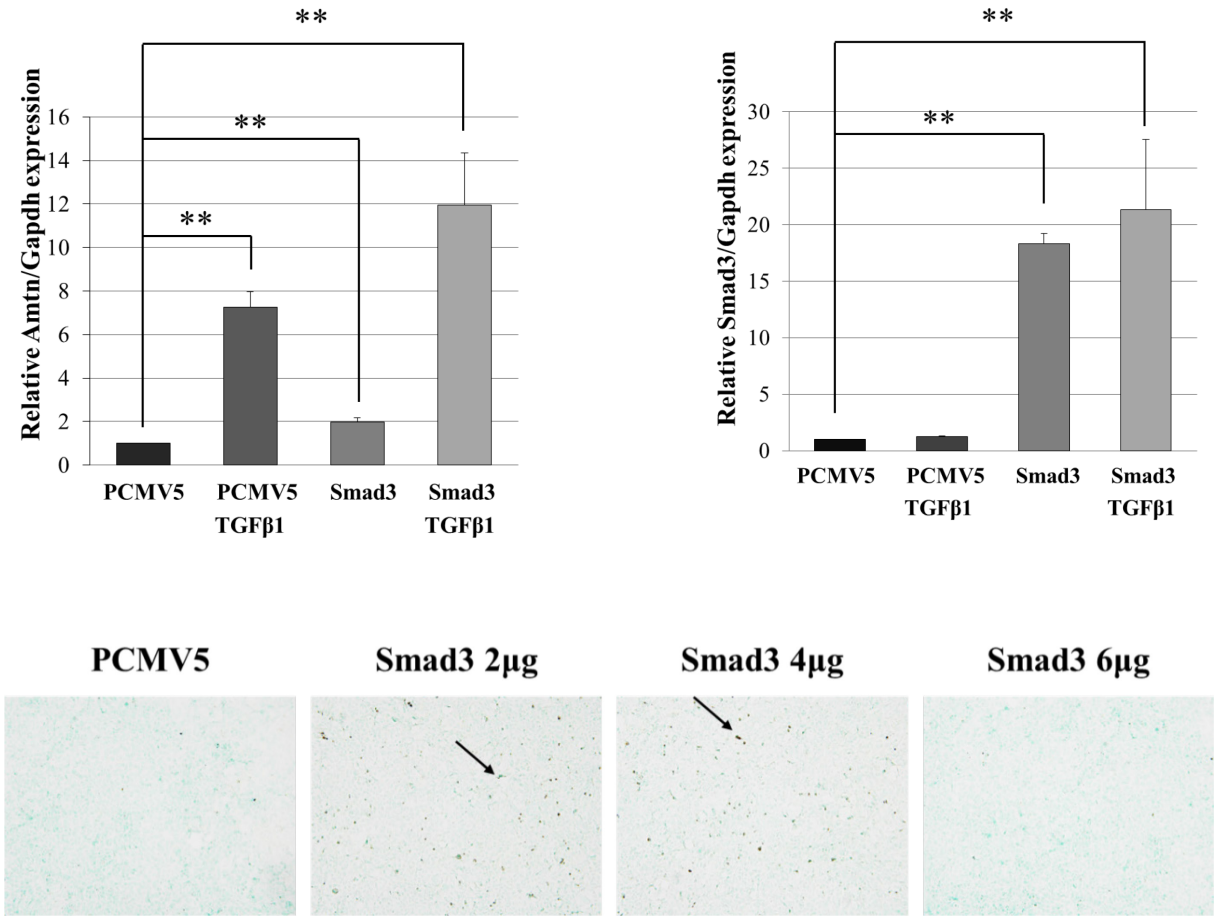

Fig. 13 Regulation of AMTN gene expression by Smad3 overexpression in GE1 cells. **A:** Overexpression of Smad3 (2 μg/ml) increased AMTN mRNA levels. The induced AMTN mRNA levels by TGFβ1 (10 ng/ml) treatment for 24 h were additionally increased by overexpression of Smad3. **B:** Smad3 expressions were significantly increased by overexpression of Smad3 (2 μg/ml) in GE1 cells. However, there were no additive effects of TGFβ1 on Smad3 expressions (**P <0.01). **C:** Smad3 overexpressions (2 and 4 μg/ml) induced an apoptosis. Weak signals of TUNEL staining were detected by 6 μg/ml Smad3 overexpression (**P <0.01).